

# **Electrophysiological Characterization of Macular Telangiectasia Type 2 (MacTel) and Structure-Function Correlation**

Mali Okada, MBBS, MMed,\* Anthony G Robson, PhD\*† Catherine A Egan,  
FRANZCO\*† Ferenc B Sallo, PhD\*† Simona Degli Esposti, MD\* Tjebo FC Heeren,  
MD\*‡ Marcus Fruttiger, PhD‡ Graham E Holder, PhD \*†

\* Moorfields Eye Hospital NHS Foundation Trust, London, UK

† UCL Institute of Ophthalmology, London, United Kingdom

‡ Department of Ophthalmology, University of Bonn, Bonn, Germany

## **Short Title:**

Electrophysiology of MacTel Type 2

## **Funding:**

Supported by the Lowy Medical Research Institute, Sydney, Australia as part of The Macular Telangiectasia Project (MO, CE). GEH receives non-specific funding from the Foundation Fighting Blindness (USA). GEH and AR also receive funding from the National Institute for Health Research (NIHR) and Biomedical Research Centre at Moorfields Eye Hospital and the University College London Institute of Ophthalmology.

## **Financial disclosures:**

None

## **Address for correspondence:**

Professor Graham E. Holder PhD

Moorfields Eye Hospital, City Road, London, United Kingdom EC1V 2PD

graham.holder@ Moorfields.nhs.uk

### **Key Words**

Macular telangiectasia type 2 (MacTel); electrophysiology; multifocal electroretinogram; pattern electroretinogram; optical coherence tomography, Müller cells

### **Summary Statement**

The electrophysiology of MacTel is consistent with a central localized disorder and an inner retinal site of dysfunction

## **Abstract**

### **Purpose**

To investigate the electrophysiological features of Macular Telangiectasia (MacTel) type 2 and their relationship to structure as determined by optical coherence tomography (OCT) imaging.

### **Methods**

Forty-two eyes from 21 patients enrolled in the MacTel Natural History Observation Study were reviewed. All patients had full-field and pattern electroretinography (ERG; PERG) with some patients additionally having multifocal electroretinography (mfERG; N=15) or electrooculography (EOG; N=12). Multiple linear regression modelling assessed the relationship between the ellipsoid zone (EZ) break size on OCT and the central mfERG response.

### **Results**

Full-field ERG and EOG were normal in all eyes. Six eyes (14%) from 5 patients had subnormal PERG P50 amplitudes. Twenty-two of 30 eyes (73%) had reduced central or paracentral stimulus on mfERG. There was a significant correlation between EZ break size and both the P1 amplitude ( $R^2 = 0.37$ ,  $p = 0.002$ ) and P1:N1 ratio ( $R^2 = 0.32$ ,  $p = 0.002$ ) of the central response on mfERG.

### **Conclusion**

The electrophysiological findings in MacTel type 2 are those of localized central dysfunction and are consistent with the structural data available from imaging and

histological studies. The EZ break size correlates with mfERG reduction. The reduced mfERG P1:N1 ratio is consistent with inner retinal dysfunction.

## **Introduction**

Macular telangiectasia (MacTel) type 2 is a bilateral slowly progressive disease of unclear aetiology characterized by macular neuro-degeneration and vascular alterations.<sup>1</sup> Typical fundoscopic findings include perifoveal graying, ectatic capillaries and crystalline deposits, with intraretinal pigment migration occurring in later stages.<sup>2</sup> Recent advances in multimodal imaging techniques have provided further morphologic characterization with evidence of hyporeflective spaces and outer retinal atrophy on optical coherence tomography (OCT), abnormal distribution of macula pigment on dual wavelength autofluorescence and increased parafoveal area of reflectance on blue light reflectance (BLR) imaging.<sup>1,3-6</sup> Emerging understanding from histological studies have pointed to localized Müller cell dysfunction and photoreceptor cell loss as central to this disorder.<sup>7</sup>

The onset of symptoms typically occurs in the fifth decade, with decline in visual acuity, development of paracentral scotomata and reading difficulty being predominant features.<sup>8-10</sup> Patients report a significant impact on vision-related quality of life early in disease, despite relatively preserved binocular distance visual acuity.<sup>8,11,12</sup> Psychophysical assessment of function with fundus-controlled perimetry (microperimetry) in mesopic conditions has identified paracentral localized scotomata.<sup>10,13</sup> Fine matrix mapping has also been used to study scotopic function, with the suggestion of greater macular rod than macular cone dysfunction in MacTel.<sup>14,15</sup> However, microperimetry and fine matrix mapping are subjective and not widely available and little is known on more objective electrophysiological measures.

Reduction in the full-field electroretinogram (ERG) responses from baseline was used as a primary safety outcome marker in a recent phase I trial for MacTel with a ciliary neurotrophic factor intraocular implant.<sup>16</sup> Electrophysiological characterization of MacTel has otherwise been limited.<sup>17-19</sup> The present study reports the electrophysiological characteristics in patients with MacTel in detail and examines possible structure/function correlation between spectral domain OCT (SD-OCT) and electrophysiological parameters.

## **Methods**

### *Study Design*

A retrospective review of patients diagnosed with MacTel type 2 at Moorfields Eye Hospital, London, UK, and who were enrolled as participants in the international MacTel Natural History Observation Study or MacTel Registry study. The protocol has been previously published with confirmation of disease status based on characteristic fundoscopy, SD-OCT, autofluorescence and fluorescein angiographic features.<sup>20</sup> All patients on the registry, who also had electrophysiology studies as part of their diagnostic work up, were identified from the hospital electronic database. Participants with other significant ocular comorbidities or with exposure to medications known to cause retinal or optic nerve toxicity were excluded from the analysis. The study was conducted according to the tenets of the Declaration of Helsinki and written informed consent was obtained from all patients.

### *Electrophysiology*

All patients underwent electrophysiological assessment using full-field and pattern electroretinography (ERG; PERG), recorded with gold foil electrodes. Pattern ERGs were recorded to a standard stimulus field (15 x 11 degrees) and additionally to a large stimulus field (30 x 22 degrees); check size was 0.8 degrees.<sup>21</sup>

Electrophysiological responses were compared with age-matched normal values and additionally for a normal level of inter-ocular symmetry (<30% difference in amplitude). A subset of patients additionally underwent multifocal ERG (mfERG) and electrooculography (EOG); this was not primarily related to clinical features, and was usually dependant upon availability of test facilities when the patient attended, but occasionally mfERG was performed if there was clinical suspicion of macular pathology but the initial PERG was normal. Protocols incorporated the standards of the International Society for Clinical Electrophysiology of Vision.<sup>22-25</sup> Multifocal ERG (RETIscan, Roland Consult, Germany) was recorded to a scaled 61 element stimulus array. The N1 (first negative) and P1 (first positive) components of the first order kernel responses were individually analyzed for the foveal field (R1) as well as the average of each of the concentric rings (R2 - 5). Paracentral responses just temporal and nasal to the central element (element 30 and 32 in a standard 61 element array) were also individually analyzed and the relative difference between the temporal versus nasal amplitudes for each eye was also compared.

#### *Optical Coherence Tomography Imaging*

Standard OCT volume scans comprising 128 B-scans within a 6x6 mm area were acquired using a Topcon 3D-OCT1000 or 3D-OCT2000 unit (Topcon Medical Systems Inc., New Jersey, United States). Segmentation and en-face imaging of the photoreceptor ellipsoid zone (EZ) line was performed using 3D image analysis

software (Visage Imaging Amira v5.3.3, Richmond, Australia). Image processing and calculation of this EZ break area in MacTel has been previously reported.<sup>26,27</sup>

Disruption of the external limiting membrane (ELM) layer on OCT was also recorded as a surrogate marker of outer retinal dysfunction.<sup>28</sup> Scaling of the mfERG waveforms for comparison to OCT was made according to the standard 61 hexagon array with the central stimulus response accounting for approximately 4.2 – 4.5°. The lower limit of 4.2° was used in the conversion of 1° to 0.28 mm for a 6 mm Topcon B-scan.

### *Statistical Analysis*

All statistical analyses were performed using the Statistical Package for the Social Sciences v.20 (IBM SPSS Inc, Chicago IL). T-test was performed to compare the means between mfERG amplitudes of patients from a group of healthy controls and in patients with and without ELM disruption. Multiple linear regression modelling was performed to examine the relationship between the size of the EZ break on en-face OCT imaging and presence of intraretinal pigment against the mfERG central hexagon response amplitude. The final model included adjustment for age, which although not significant on univariate modelling, may affect the electrophysiological responses. A value of  $p < 0.05$  was considered significant.

## **Results**

### *Patient Characteristics*

A total of 23 patients with MacTel on the registry had electrophysiological studies. One was excluded from the final analysis because of unexplained light perception visual acuity not consistent with MacTel; the other had been treated with hydroxychloroquine for rheumatoid arthritis. Of the remaining 21 patients, the

average age was  $58.7 \pm 10.6$  years and the majority were female ( $n = 15, 71\%$ ) (Table 1). Mean visual acuity at the time of electrophysiological testing was logMAR  $0.41 \pm 0.21$ , equivalent to 20/51 Snellen visual acuity. All 42 eyes were treatment naïve. No patients had subretinal neovascularization or macular hole complications secondary to MacTel.

### *Electrophysiology*

Full-field ERG and PERG were performed in all patients. Full-field ERGs (comprising ISCEV DA0.01, DA10.0, LA30Hz and LA3.0 responses) were normal for age in all 42 eyes (Table 2). Six of 42 eyes (14%) had subnormal PERG P50 amplitudes either compared to the lower limits of normal for age ( $n = 5$ ) or as compared to the fellow eye with significant interocular asymmetry of more than 30% ( $n = 1$ ) (see Figure 1). With a doubled stimulus field, the P50 amplitude increased by a mean 2.85 times (range 2.5 – 3.7) in patients with subnormal response to standard field (lower limit of normal enlargement 60%).<sup>21</sup> The mean P50 amplitudes for the cohort were within normal limits for age (Table 2).

Multifocal ERG responses are displayed in Figure 2. Twenty-two of 30 eyes (73%) had reduction in the first positive response (P1) amplitude but accompanied by preservation of the first negative (N1) amplitude for the central hexagon, resulting in a reduced P1:N1 ratio. The dysfunction was highly localized, affecting the central or paracentral responses and sparing the outer elements (Figure 3). When compared to a control group, the P1:N1 ratio from the central response was significantly different from normal (mean ratio:  $2.5 \pm 1.0$  vs.  $3.0 \pm 0.4$ ,  $p = 0.003$  respectively) (Table 3). The P1:N1 ratio was not statistically different in any other ring. There was reduced

paracentral response in 15 eyes (50%): 13 of which were confined to the temporal paracentral element and 2 eyes where the dysfunction affected most of the paracentral ring (R2). There was significant asymmetry between temporal and nasal paracentral responses, with a mean  $26 \pm 16\%$  reduction in the temporal P1 amplitude as compared to the nasal response (Figure 4). All eyes with a normal mfERG (n=8) also had a normal PERG P50 component.

There was no statistically significant difference in the central mfERG P1 response in the patients with and without intraretinal pigment migration on multiple linear regression analysis controlling for age (central P1 amplitude:  $B = -0.22$ ,  $p = 0.17$ ,  $R^2 = 0.03$ ). There was a trend towards significance for the central P1:N1 ratio ( $B = -0.46$ ,  $p = 0.07$ ,  $R^2 = 0.11$ ) but the effect size was small. There was also no difference in the PERG P50 component between the two groups.

EOGs were normal in all those tested (n= 24 eyes; mean light rise:  $258 \pm 74\%$ ).

#### *Correlation between mfERG and Optical Coherence Tomography*

OCT in all patients revealed inner retinal hyporeflective cavitations and/or changes in reflectivity in keeping with neurodegeneration and consistent with MacTel. In the subset that had mfERG, 27 eyes (90%) had an EZ break on OCT (mean  $1.2 \pm 1.3$  mm<sup>2</sup>, range 0 – 4.4 mm<sup>2</sup>) and 20 eyes (67%) had disruption of the ELM on B-scan.

The central and paracentral responses on mfERG were compared against the area of EZ loss on OCT (Figure 5). Linear regression modelling examined the correlation between the EZ break size on imaging and the mfERG response. Age and eye laterality were not significant predictors on univariate analysis. Increasing size of the EZ break area was significantly associated with decreasing central hexagon P1 amplitudes on multiple regression analysis controlling for age ( $R^2 = 0.37$ , Beta coefficient =  $-0.26$ ,  $p = 0.002$ ). Similarly, increasing size of the EZ break area was also predictive of a greater decrease in central P1:N1 ratio ( $R^2 = 0.32$ , Beta coefficient =  $-0.51$ ,  $p = 0.002$ ), Figure 6. There was no significant association with any of the ring averaged peripheral responses. Further analysis of the five eyes that had either no EZ break on any slice ( $n=3$ ) or only a very small EZ break with an area  $< 0.05\text{mm}^2$  ( $n=2$ ) revealed evidence of subnormal central stimulus in all but one, with mean central P1 amplitude of  $1.1 \pm 0.4 \mu\text{V}$  but less apparent reduction in the P1:N1 ratio ( $2.8 \pm 0.7 \mu\text{V}$ ).

The localized reduction in the first positive response and preservation of the first negative response was even more pronounced in patients with concurrent outer retinal disease as assessed by disruption of the ELM ( $n = 20$ , 67%) (Figure 7). The mean P1:N1 ratio of the central hexagon was  $2.8 \pm 0.6$  when the ELM was intact vs.  $2.2 \pm 0.7$  when the ELM was disrupted,  $t(28) = 2.5$ ,  $p = 0.02$ ). However, there was no difference in the absolute amplitude of the first positive response (P1) between eyes with or without an intact ELM (mean  $1.3 \pm 0.4 \mu\text{V}$  vs.  $1.1 \pm 0.4 \mu\text{V}$ ,  $t(28) = 1.1$ ,  $p = 0.28$ ). No significant difference in responses was present in the periphery.

## **Discussion**

This study provides comprehensive functional assessment of MacTel using electrophysiology, significantly extending previous limited reports. It further demonstrates a novel structure/function correlation between electrophysiological parameters and structural neurodegeneration as shown on OCT imaging.

In the early descriptions of the disease by Gass and Oyakawa<sup>17</sup>, three patients from group 3 idiopathic juxtafoveolar telangiectasia (equivalent to MacTel type 2) had ERG and EOG performed. Data and protocol were not detailed but results were reported to be normal. In contrast, a later case was described of a patient with MacTel who was initially presumed to have a cone dystrophy due to cone dysfunction on electrophysiology (reduced LA30Hz and LA3.0 ERG).<sup>18</sup> The present results are in keeping with the original 3 cases presented by Gass and Oyakawa with full-field electroretinography normal in every patient, and thus, no evidence of generalized retinal dysfunction. Similarly, the preserved EOG light rise suggests there to be no generalized disturbance of RPE function. Pattern ERG P50 was mildly subnormal in a small proportion of patients to standard field stimulus but showed normal enlargement to a large field stimulus, in keeping with the mfERG evidence of localized central macular dysfunction.

In the majority of cases, mfERGs showed preservation of the early negative component (N1) in the response to the central stimulus element but selective reduction of the positive component (P1); in healthy normal subjects, the central response is usually the largest in the array. The temporal paracentral response was also affected in half of the patients, with significant asymmetry between temporal and nasal response. Peripheral mfERG responses were unaffected. These data support the

concept of MacTel having localized disturbance of macular function, and uniquely provide evidence of an inner retinal site of dysfunction.

Understanding of the pathological MacTel area has increased with the advent of advanced imaging techniques. The initial classification of MacTel in the early 1990s described a juxtafoveal area of telangiectasis as seen on biomicroscopy and paracentral late phase hyperfluorescence on fluorescein angiography.<sup>2</sup> More recently however, confocal BLR imaging has revealed a characteristic pattern of oval paracentral hyper-reflectance that is usually slightly larger than the angiographic area of leakage.<sup>4,29</sup> This reflectance phenomenon shares topographic correlation with the focal area of central macular pigment reduction seen with dual wavelength autofluorescence.<sup>5</sup> Evidence for this discrete MacTel area is also present from histopathology; a marked area of macular pigment loss centrally was present on macroscopic pathological examination of a donor MacTel eye.<sup>7</sup> There was reported to be an oval boundary with an approximate 6.5° horizontal by 5° vertical dimension,<sup>1,5,30</sup> consistent with measurements of abnormal annular macular pigment in MacTel on dual wavelength autofluorescence (median peak optical density at approximately 5.2° eccentricity). This is also in keeping with the present mfERG data, showing dysfunction confined to the central or paracentral area (the central response element corresponds to ~4.5° horizontal diameter in a 61 element array).

There was also significant temporal and nasal asymmetry in this cohort. In eyes with paracentral involvement, the temporal paracentral element was a mean 25% lower in P1 amplitude when compared to the nasal side. An epicentre of the disease temporal to the fovea is also suggested from previous studies with retinal changes presenting

temporally initially on fundus examination,<sup>31</sup> as well on imaging<sup>1,32</sup> and functional assessment with microperimetry.<sup>10</sup> This asymmetry and localized temporal paracentral involvement may also explain the normal results for R2 in this cohort as compared to normals, as the dysfunction is diluted out when taking averages of all the responses in the paracentral ring. The focal reduction in the temporal paracentral response is all the more striking as previous studies have suggested that the naso-temporal difference is reversed in normal eyes, with the temporal response usually slightly greater than the nasal.<sup>33,34</sup>

The highly localized nature of the disease also explains the normal PERG response in the majority of the patients, since the PERG arises from a 15x12° central area<sup>35</sup> and lacks the spatial resolution of the mfERG to detect small localized areas of dysfunction. However, it should be noted that mfERG testing is highly dependent on the ability of the patient to fixate accurately and PERG may prove informative in patients unable to fixate optimally.

Yellow foveal subretinal deposits have been described in a small case series of MacTel patients.<sup>17,36</sup> The material consisted of degenerate photoreceptor outer segments on electron microscopy with corresponding hyperautofluorescence on imaging. Unlike foveomacular vitelliform dystrophy, there was no reported associated retinal pigment epithelium (RPE) reaction microscopically. More widespread subretinal deposits have also been reported on histologic examination, consisting of photoreceptor outer segments and RPE proteins.<sup>37</sup> None of the present patients, however, had evidence of any yellow lesion on fundoscopy or on imaging. The

normal EOGs and full-field ERGs in the present cohort argue against widespread RPE dysfunction and support the subclinical nature of these histologic findings.

The finding of a reduced P1:N1 ratio in the central mfERG recording, resulting from a selective reduction in the positive component of the response, suggests inner retinal dysfunction localized to the central macula.<sup>33,38,39</sup> Although the exact pathogenesis of the disorder is still to be determined, immunohistochemistry in confirmed cases of MacTel showed central loss of reactivity of Müller cell markers in the same distribution as the macular pigment loss.<sup>7,40</sup> It was hypothesized that MacTel may be a primary Müller cell disorder<sup>7,36</sup> and that the neurodegenerative features of this disease may be a consequence of the Müller cell role in neuroprotection and recycling of toxic neurotransmitters.<sup>41,42</sup>

The mfERG P1 amplitudes and P1:N1 ratios correlated with the size of EZ disruption on en-face OCT in this study. Natural history studies have demonstrated progressive neurodegeneration in MacTel as evidenced by expansion in the area of EZ hyporeflectivity on OCT imaging.<sup>27</sup> The electrophysiological responses here support data from previous microperimetry studies,<sup>26,27</sup> additionally providing objective structure-function correlation and localising dysfunction to a level that is inner retinal. It may also give an indication of the lateral extent of inner retinal dysfunction as reduction in central mfERG response was seen even in eyes without an EZ break.

It has recently been reported that localised visual function may still be present in MacTel eyes in areas where cones are not visualized on imaging. Using adaptive optics scanning laser ophthalmoscopy (AOSLO) and AOSLO integrated

microperimetry (AOMP), retinal sensitivity was shown to be retained, albeit at a higher threshold, in some areas of EZ hyporeflectivity on OCT imaging if the ELM was intact.<sup>28</sup> Interestingly, in the present cohort, evidence of ELM disruption was associated with even greater reduction in the P1:N1 amplitude in the central hexagon compared to those with an intact ELM layer. Typically, a normal P1:N1 ratio would be expected in primary photoreceptor disease.<sup>38</sup> The finding here of a reduced P1:N1 ratio therefore suggests that even in the presence of photoreceptor abnormalities on imaging, the primary pathology in these patients is post-synaptic to photoreceptors. The greater reduction in the ratio seen in patients with an ELM break may reflect the patients with more advanced disease and therefore greater inner retinal dysfunction. Similarly there was no direct correlation between presence of intraretinal pigment migration and the mfERG central response amplitude. There was a trend however towards reduced central P1:N1 ratio. Larger number of patients may determine if this is significant.

The localized findings in the present cohort are in contrast with the only other reported mfERG data in MacTel<sup>19</sup>. Those authors published results from 14 patients with a diagnosis of MacTel based on clinical examination and fundus fluorescein angiogram. Patients underwent mfERG studies only, using a similar 61-stimulus array. Global macular dysfunction was described and reduction in amplitudes was reported in both P1 and N1 components. The greatest changes were seen in the central responses < 2° but both N1 and P1 were reported abnormal even in eccentric responses. The difference in outcomes between the two studies may be due to differences in study population. The present cohort had MacTel confirmed by multimodal imaging including not only fluorescein angiography but also SD-OCT

and autofluorescence. It should be noted that those authors acknowledged technical difficulties and the presence of artefacts, and further interpreted the result as percentage reduction instead of assessment of each waveform. Those factors may be relevant given the known dependence of any electrophysiological measure, but particularly mfERG, on technical factors and fixation.

A limitation of this study is that as it was retrospective, not all patients in the series had mfERG or EOG performed. However the subset who had additional mfERG testing covered the spectrum of MacTel disease severity from small inner retinal hyporeflective cavities without outer retinal pathology to patients with severe foveal atrophy and intraretinal pigment migration. Further, it also included patients who had both normal and subnormal responses on initial PERG.

## **Conclusion**

This study provides a comprehensive electrophysiological characterization of retinal and macular function in MacTel. The majority of cases show dysfunction, detected in most by mfERG testing and invariably confined to the central macular area. The nature of the mfERG changes support an inner retinal site of dysfunction, potentially related to abnormal Müller cell function, and the size of the mfERG response can be correlated with structural changes of ellipsoid zone loss evident on OCT. In contrast with previous reports, no generalized mfERG abnormalities were detected in this cohort. The study highlights the utility of mfERG testing in MacTel, showing high sensitivity and exposing evidence of highly localized inner retinal dysfunction, not revealed by PERG.

Dual-wavelength autofluorescence for macular pigment optical density mapping is not readily available and patients are often referred for electrophysiological testing with unspecified macular pathology and the diagnosis of MacTel not necessarily suspected. Although the pattern of reduced positivity in the central and temporal paracentral hexagons on mfERG is not disease specific, such findings may be a useful non-invasive adjunct to multimodal imaging in cases of diagnostic uncertainty. Furthermore, electrophysiological testing may be a useful objective method of assessing function for monitoring of disease progression in an individual patient or as an endpoint in therapeutic clinical trials.

## References

1. Charbel Issa P, Gillies MC, Chew EY, et al. Macular telangiectasia type 2. *Prog Retin Eye Res* 2013;34:49–77.
2. Gass JD, Blodi BA. Idiopathic juxtafoveolar retinal telangiectasis. Update of classification and follow-up study. *Ophthalmology* 1993;100:1536–1546.
3. Sallo FB, Leung I, Clemons TE, et al. Multimodal imaging in type 2 idiopathic macular telangiectasia. *Retina* 2015;35:742–749.
4. Charbel Issa P, Berendschot TTJM, Staurenghi G, et al. Confocal blue reflectance imaging in type 2 idiopathic macular telangiectasia. *Invest Ophthalmol Vis Sci* 2008;49:1172–1177.
5. Charbel Issa P, van der Veen RLP, Stijfs A, et al. Quantification of reduced macular pigment optical density in the central retina in macular telangiectasia type 2. *Exp Eye Res* 2009;89:25–31.
6. Degli Esposti S, Egan C, Bunce C, et al. Macular pigment parameters in patients with macular telangiectasia (MacTel) and normal subjects: implications of a novel analysis. *Invest Ophthalmol Vis Sci* 2012;53:6568–6575.
7. Powner MB, Gillies MC, Zhu M, et al. Loss of Muller's cells and photoreceptors in macular telangiectasia type 2. *Ophthalmology* 2013;120:2344–2352.
8. Heeren TFC, Holz FG, Charbel Issa P. First symptoms and their age of onset in macular telangiectasia type 2. *Retina* 2014;34:916–919.
9. Finger RP, Charbel Issa P, Fimmers R, et al. Reading performance is reduced by parafoveal scotomas in patients with macular telangiectasia type 2. *Invest Ophthalmol Vis Sci* 2009;50:1366–1370.
10. Charbel Issa P, Helb H-M, Rohrschneider K, et al. Microperimetric assessment of patients with type 2 idiopathic macular telangiectasia. *Invest Ophthalmol Vis Sci* 2007;48:3788–3795.
11. Lamoureux EL, Maxwell RM, Marella M, et al. The longitudinal impact of macular telangiectasia (MacTel) type 2 on vision-related quality of life. *Invest Ophthalmol Vis Sci* 2011;52:2520–2524.
12. Clemons TE, Gillies MC, Chew EY, et al. The National Eye Institute Visual Function Questionnaire in the Macular Telangiectasia (MacTel) Project. *Invest Ophthalmol Vis Sci* 2008;49:4340–4346.
13. Heeren TFC, Clemons T, Scholl HPN, et al. Progression of Vision Loss in Macular Telangiectasia Type 2. *Invest Ophthalmol Vis Sci* 2015;56:3905–3912.
14. Schmitz-Valckenberg S, Fan K, Nugent A, et al. Correlation of functional impairment and morphological alterations in patients with group 2A idiopathic

juxtafoveal retinal telangiectasia. Arch Ophthalmol Chic Ill 1960 2008;126:330–335.

15. Schmitz-Valckenberg S, Ong EEL, Rubin GS, et al. Structural and functional changes over time in MacTel patients. Retina 2009;29:1314–1320.

16. Chew EY, Clemons TE, Peto T, et al. Ciliary neurotrophic factor for macular telangiectasia type 2: results from a phase 1 safety trial. Am J Ophthalmol 2015;159:659–666.e1.

17. Gass JD, Oyakawa RT. Idiopathic juxtafoveolar retinal telangiectasis. Arch Ophthalmol Chic Ill 1960 1982;100:769–780.

18. Barthelmes D, Gillies MC, Fleischhauer JC, Sutter FKP. A case of idiopathic perifoveal Telangiectasia preceded by features of cone dystrophy. Eye Lond Engl 2007;21:1534–1535.

19. Narayanan R, Dave V, Rani PK, et al. Multifocal electroretinography in type 2 idiopathic macular telangiectasia. Graefes Arch Clin Exp Ophthalmol Albrecht Von Graefes Arch Klin Exp Ophthalmol 2013;251:1311–1318.

20. Clemons TE, Gillies MC, Chew EY, et al. Baseline characteristics of participants in the natural history study of macular telangiectasia (MacTel) MacTel Project Report No. 2. Ophthalmic Epidemiol 2010;17:66–73.

21. Lenassi E, Robson AG, Hawlina M, Holder GE. The value of two-field pattern electroretinogram in routine clinical electrophysiologic practice. Retina 2012;32:588–599.

22. Bach M, Brigell MG, Hawlina M, et al. ISCEV standard for clinical pattern electroretinography (PERG): 2012 update. Doc Ophthalmol Adv Ophthalmol 2013;126:1–7.

23. Hood DC, Bach M, Brigell M, et al. ISCEV standard for clinical multifocal electroretinography (mfERG) (2011 edition). Doc Ophthalmol Adv Ophthalmol 2012;124:1–13.

24. Marmor MF, Brigell MG, McCulloch DL, et al. ISCEV standard for clinical electro-oculography (2010 update). Doc Ophthalmol Adv Ophthalmol 2011;122:1–7.

25. McCulloch DL, Marmor MF, Brigell MG, et al. Erratum to: ISCEV Standard for full-field clinical electroretinography (2015 update). Doc Ophthalmol Adv Ophthalmol 2015;131:81–83.

26. Sallo FB, Peto T, Egan C, et al. “En face” OCT imaging of the IS/OS junction line in type 2 idiopathic macular telangiectasia. Invest Ophthalmol Vis Sci 2012;53:6145–6152.

27. Sallo FB, Peto T, Egan C, et al. The IS/OS junction layer in the natural history of type 2 idiopathic macular telangiectasia. *Invest Ophthalmol Vis Sci* 2012;53:7889–7895.
28. Wang Q, Tuten WS, Lujan BJ, et al. Adaptive optics microperimetry and OCT images show preserved function and recovery of cone visibility in macular telangiectasia type 2 retinal lesions. *Invest Ophthalmol Vis Sci* 2015;56:778–786.
29. Charbel Issa P, Finger RP, Helb H-M, et al. A new diagnostic approach in patients with type 2 macular telangiectasia: confocal reflectance imaging. *Acta Ophthalmol (Copenh)* 2008;86:464–465.
30. Helb H-M, Charbel Issa P, VAN DER Veen RLP, et al. Abnormal macular pigment distribution in type 2 idiopathic macular telangiectasia. *Retina* 2008;28:808–816.
31. Abujamra S, Bonanomi MT, Cresta FB, et al. Idiopathic juxtafoveal retinal telangiectasis: clinical pattern in 19 cases. *Ophthalmol J Int Ophtalmol Int J Ophthalmol Z Augenheilkd* 2000;214:406–411.
32. Barthelmes D, Gillies MC, Sutter FKP. Quantitative OCT analysis of idiopathic perifoveal telangiectasia. *Invest Ophthalmol Vis Sci* 2008;49:2156–2162.
33. Hood DC. Assessing retinal function with the multifocal technique. *Prog Retin Eye Res* 2000;19:607–646.
34. Parks S, Keating D, Williamson TH, et al. Functional imaging of the retina using the multifocal electroretinograph: a control study. *Br J Ophthalmol* 1996;80:831–834.
35. Holder GE. Pattern electroretinography (PERG) and an integrated approach to visual pathway diagnosis. *Prog Retin Eye Res* 2001;20:531–561.
36. Cherepanoff S, Killingsworth MC, Zhu M, et al. Ultrastructural and clinical evidence of subretinal debris accumulation in type 2 macular telangiectasia. *Br J Ophthalmol* 2012;96:1404–1409.
37. Powner MB, Gillies MC, Zhu M, et al. Pan-retinal, subretinal aggregates in Macular Telangiectasia Type 2. *Invest Ophthalmol Vis Sci* 2014;55:6320–6320.
38. Hood DC, Seiple W, Holopigian K, Greenstein V. A comparison of the components of the multifocal and full-field ERGs. *Vis Neurosci* 1997;14:533–544.
39. Hasegawa S, Ohshima A, Hayakawa Y, et al. Multifocal Electroretinograms in Patients with Branch Retinal Artery Occlusion. *Invest Ophthalmol Vis Sci* 2001;42:298–304.
40. Powner MB, Gillies MC, Tretiach M, et al. Perifoveal muller cell depletion in a case of macular telangiectasia type 2. *Ophthalmology* 2010;117:2407–2416.

41. Bringmann A, Iandiev I, Pannicke T, et al. Cellular signaling and factors involved in Muller cell gliosis: neuroprotective and detrimental effects. *Prog Retin Eye Res* 2009;28:423–451.
42. Bringmann A, Pannicke T, Biedermann B, et al. Role of retinal glial cells in neurotransmitter uptake and metabolism. *Neurochem Int* 2009;54:143–160.

**Table 1.** Patient Demographics

<b>Characteristic</b>	<b>Value</b>
Patients (n)	21
Eyes (n)	42
Age (y)	
Mean $\pm$ SD	58.7 $\pm$ 10.6
Range	39 – 74
Female, n (%)	15 (71)
Best corrected visual acuity	
Mean $\pm$ SD (LogMAR)	0.41 $\pm$ 0.21
Mean Snellen Acuity	20/51
LogMAR Range (Snellen)	-0.08 – 1.00 (20/17 – 20/200)

SD: standard deviation;

**Table 2.** Summary of electrophysiological responses in MacTel patients performed according to ISCEV standard. Normal limits for the two age groups are defined as the minimum normal amplitude minus 5% of the reference interval (maximum normal value – minimum normal value) in a healthy cohort.

	<b>MacTel</b> <b>(m±SD μV)</b>	<b>Normal Limits</b> <b>(μV)</b>
<b>ERG</b>		
Age < 50 (n=10)		
DA 0.01	289 ± 53 (235 – 365)	> 140
DA 10.0 a-wave	354 ± 45 (260 – 410)	> 240
DA 10.0 b-wave	575 ± 98 (415 – 700)	> 350
LA 3.0 b-wave	166 ± 29 (120 – 205)	>101
LA 30Hz flicker	107 ± 14 (85 – 135)	> 70
Age ≥ 50 (n = 32)		
DA 0.01	220 ± 71 (100 – 370)	> 80
DA 10.0 a-wave	309 ± 54 (180 – 400)	> 150
DA 10.0 b-wave	452 ± 72 (240 – 645)	> 200
LA 3.0 b-wave	143 ± 31 (99 – 190)	> 95
LA 30Hz flicker	104 ± 29 (65 – 170)	> 62
<b>PERG</b>		
Age < 50 (n = 10)		
P50 amp	2.7 ± 0.5 (2.1 – 3.7)	> 2.0
Age ≥ 50 (n = 32)		
P50 amp	2.3 ± 0.7 (1.0 – 4.2)	> 1.5
<b>EOG</b>		
Number of eyes (%)	24 (57)	
Light rise %, m±SD	258 ± 74	> 180

μV: microvolts; ERG : full-field electroretinogram ; DA: dark-adapted; LA: light-adapted; PERG : pattern electroretinogram; EOG : electrooculogram

**Table 3.** Central multifocal electroretinogram responses in MacTel compared to a healthy control cohort

<b>Parameters</b>	<b>MacTel (n = 30)</b>	<b>Controls (n = 12)</b>	<b>P-value</b>
Central stimulus N1 amplitude, m±SD (μV)	0.4 ± 0.2	0.7 ± 0.1	0.08
Central stimulus P1 amplitude, m±SD (μV)	1.2 ± 0.5	2.4 ± 0.7	< 0.01*
Central P1:N1 ratio, m±SD	2.5 ± 1.0	3.0 ± 0.4	<0.01*
Central stimulus N1 latency, m±SD (ms)	19.0 ± 3.7	18.2 ± 2.0	0.49
Central stimulus P1 latency, m±SD (ms)	39.4 ± 5.9	42.7 ± 2.7	0.08

m: mean; SD: standard deviation; μV: microvolts ; ms = millisecond

**Figure 1.**  
Pattern electroretinogram P50 amplitudes in MacTel 2 compared to controls

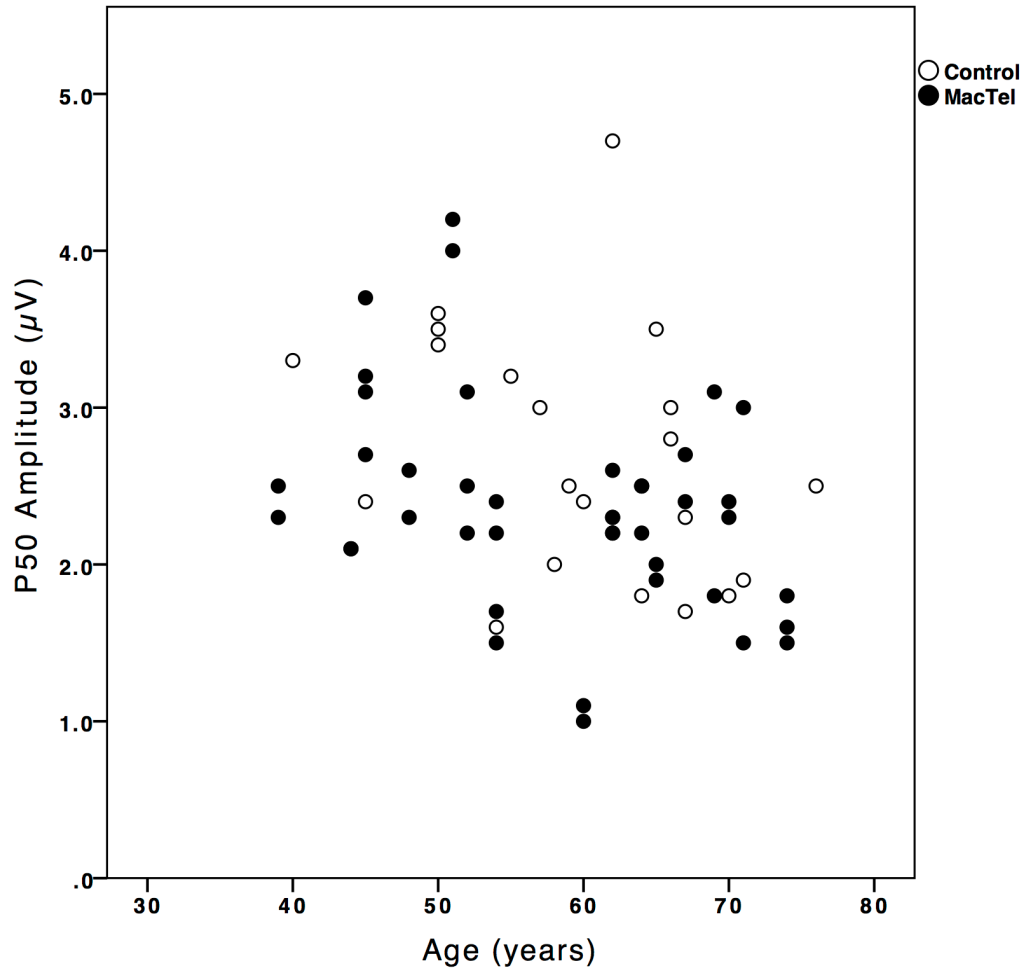


**Figure 2.**

Multifocal electroretinogram of the right eye of a 62 year old female with MacTel 2 demonstrating preserved first negative response (N1) and reduced first positive response (P1) in central element (arrow). Inset - Enlarged view of above comparing central element waveform (left) and a more peripheral waveform (right). In healthy subjects, the central element is usually the largest.

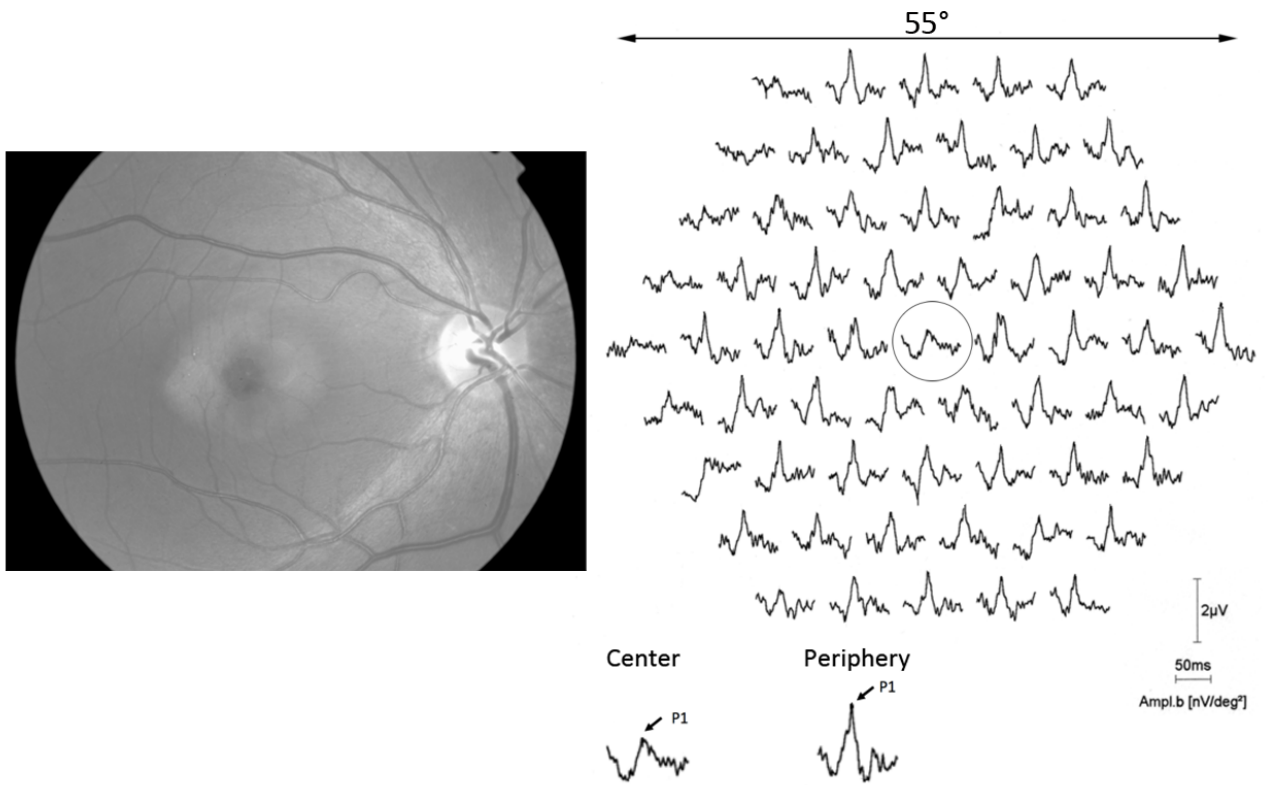


**Figure 3.** Multifocal electroretinography (mfERG) P1:N1 ratio by rings in MacTel patients compared to control group. Results displayed as boxplot.

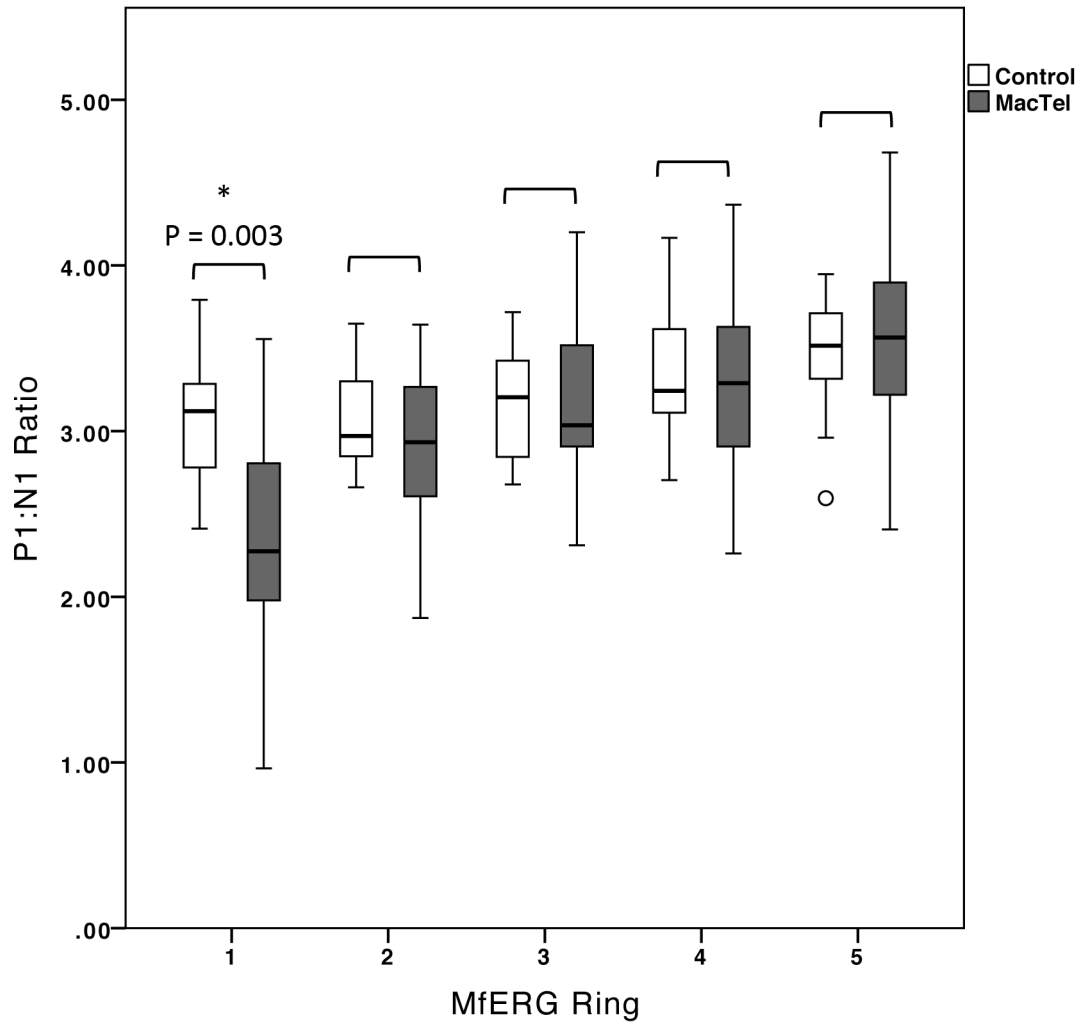


**Figure 4.**

Multifocal electroretinogram of the right eye of a 74 year old man with MacTel 2 revealing temporal parafoveal reduction compared to nasal parafoveal response. Corresponding fundus image with area of ellipsoid zone loss outlined on enface imaging.

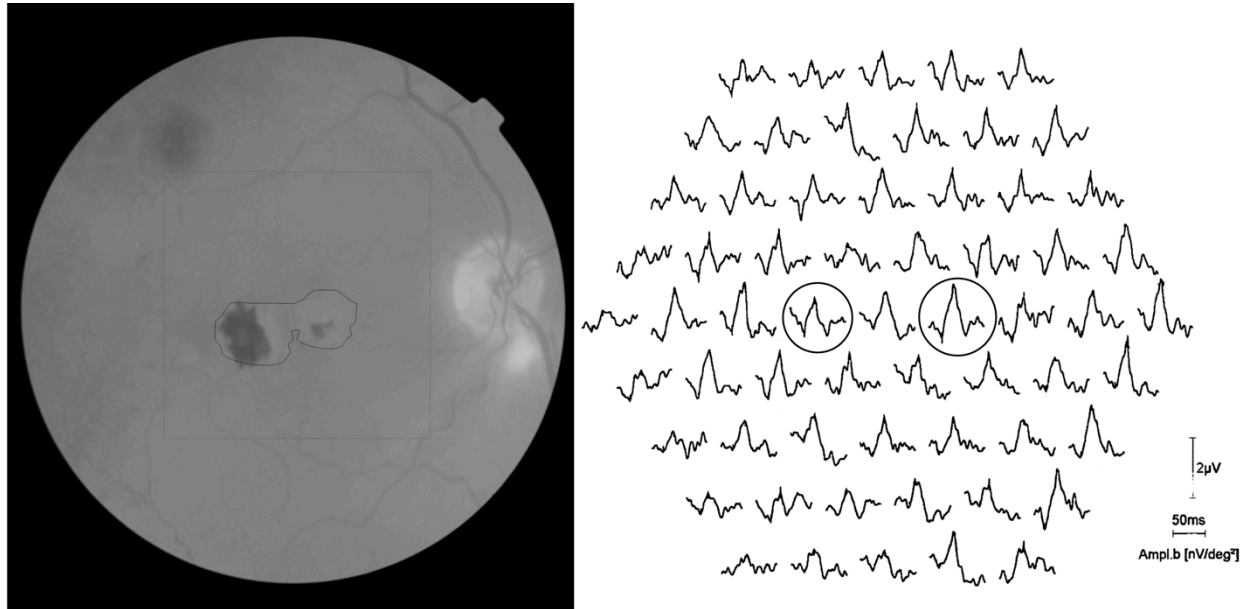


**Figure 5.**

Mapping of multifocal electroretinogram central and paracentral stimulus elements against optical coherence tomography scans in a 70 year old female. Left: En-face image of area of ellipsoid zone break; Right: Corresponding B-scan image with scaled waveforms (1mm = 3.57°)

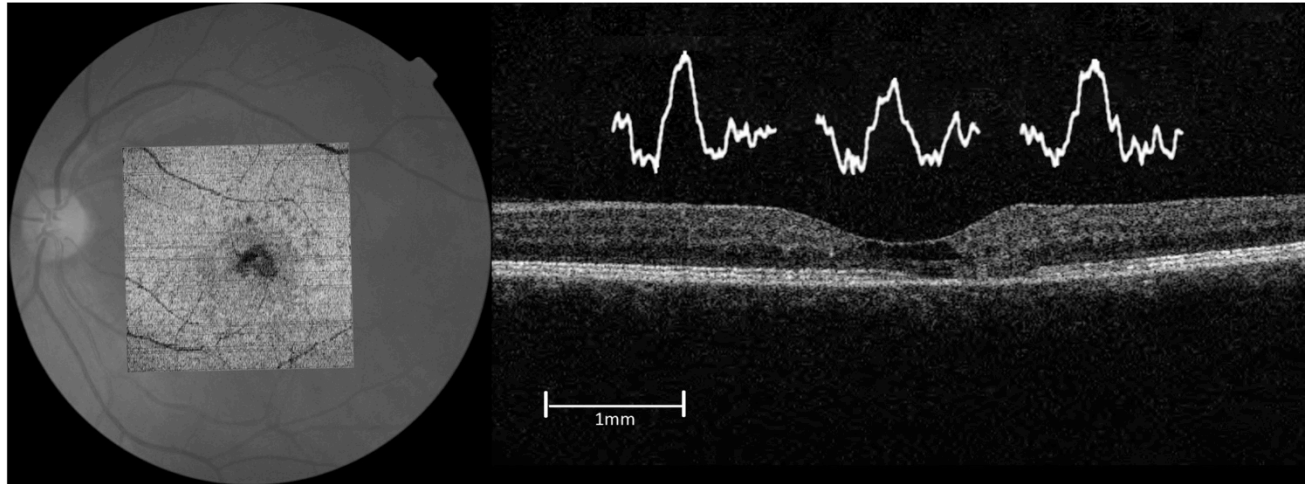


**Figure 6.**

Correlation between ellipsoid zone break with (A) central response P1 amplitude in multifocal electroretinography (mfERG) and (B) central response P1:N1 ratio.

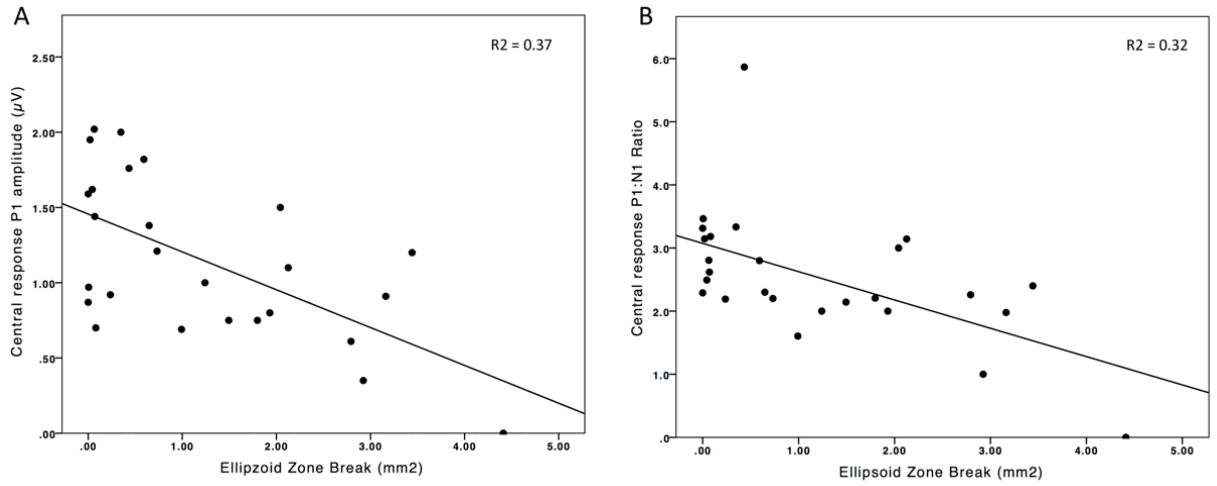


**Figure 7.**

64 year old female with MacTel 2. Left visual acuity 20/120 with outer retinal atrophy on optical coherence tomography. Multifocal electroretinogram demonstrates reduced P1:N1 ratio in central element.

